NASA/TM—1999-209076

Sliding Wear and Fretting Wear of DLC-Based, Functionally Graded Nanocomposite Coatings

K. Miyoshi, B. Pohlchuck, and Kenneth W. Street
Glenn Research Center, Cleveland, Ohio

J.S. Zabinski, J.H. Sanders, and A.A. Voevodin
Air Force Research Laboratory, Wright-Patterson Air Force Base, Ohio

R.L.C. Wu
K Systems Corp., Beavercreek, Ohio

National Aeronautics and
Space Administration

Glenn Research Center

May 1999

Acknowledgments

The authors would like to thank Jerry Pobuda of Cortez for the experimental setups, Duane J. Dixon of Vehicle Technology Center for SEM, and Rifka Cohen of Kent State University for wear measurements.

Available from

NASA Center for Aerospace Information
7121 Standard Drive
Hanover, MD 21076
Price Code: A03

National Technical Information Service
5285 Port Royal Road
Springfield, VA 22100
Price Code: A03

SLIDING WEAR AND FRETTING WEAR OF DLC-BASED, FUNCTIONALLY GRADED NANOCOMPOSITE COATINGS

K. Miyoshi, B. Pohlchuck, and K.W. Street
National Aeronautics and Space Administration
Glenn Research Center
Cleveland, Ohio 44135

J.S. Zabinski, J.H. Sanders, and A.A. Voevodin
Air Force Research Laboratory
Wright-Patterson Air Force Base, Ohio 45433

R.L.C. Wu
K Systems Corp.
Beavercreek, Ohio 45432

SUMMARY

Improving the tribological functionality of diamondlike carbon (DLC) films—developing good wear resistance, low friction, and high load-carrying capacity—was the aim of this investigation. Nanocomposite coatings consisting of an amorphous DLC (a-DLC) top layer and a functionally graded titanium–titanium carbon–diamondlike carbon (Ti-Ti_xC_y-DLC) underlayer were produced on AISI 440C stainless steel substrates by the hybrid technique of magnetron sputtering and pulsed-laser deposition. The resultant DLC films were characterized by Raman spectroscopy, scanning electron microscopy, and surface profilometry. Two types of wear experiment were conducted in this investigation: sliding friction experiments and fretting wear experiments. Unidirectional ball-on-disk sliding friction experiments were conducted to examine the wear behavior of an a-DLC/Ti-Ti_xC_y-DLC-coated AISI 440C stainless steel disk in sliding contact with a 6-mm-diameter AISI 440C stainless steel ball in ultrahigh vacuum, dry nitrogen, and humid air. Although the wear rates for both the coating and ball were low in all three environments, the humid air and dry nitrogen caused mild wear with burnishing in the a-DLC top layer, and the ultrahigh vacuum caused relatively severe wear with brittle fracture in both the a-DLC top layer and the Ti-Ti_xC_y-DLC underlayer. For reference, amorphous hydrogenated carbon (H–DLC) films produced on a-DLC/Ti-Ti_xC_y-DLC nanocomposite coatings by using an ion beam were also examined in the same manner. The H–DLC films markedly reduced friction even in ultrahigh vacuum without sacrificing wear resistance. The H–DLC films behaved much like the a-DLC/Ti-Ti_xC_y-DLC nanocomposite coating in dry nitrogen and humid air, presenting low friction and low wear. Fretting wear experiments were conducted in humid air (~50 percent relative humidity) at a frequency of 80 Hz and an amplitude of 75 μm on an a-DLC/Ti-Ti_xC_y-DLC-coated AISI 440C disk and on a titanium–6 wt% aluminum–4 wt% vanadium (Ti-6Al-4V) flat, both in contact with a 9.4-mm-diameter, hemispherical Ti-6Al-4V pin. The resistance to fretting wear and damage of the a-DLC/Ti-6Al-4V materials pair was superior to that of the Ti-6Al-4V/Ti-6Al-4V materials pair.

INTRODUCTION

The nature of the substrate and its predeposition treatment play a major role in determining the load-carrying capacity and wear resistance of diamondlike carbon (DLC) coatings in tribological applications. Especially when the DLC coatings are applied to relatively soft substrates, such as steels, the brittle nature and high internal compressive stresses (1 to 2 GPa) of DLC may limit the applications to light loads. In other words, the maximum load that such a sliding or rolling contact system can support without failure or wear exceeding the design limits for the particular application is low. Therefore, the synergistic characteristics of amorphous DLC (a-DLC), such as bending strength, shear strength, elasticity, and hardness, as well as adhesion of DLC to its substrate in DLC-substrate systems, must be improved through methods such as the use of multilayer DLC coatings (refs. 1 to 8) and compositional modification of DLC (refs. 9 to 14).

In a previous study by Voevodin et al. (ref. 1) several design concepts, including titanium–titanium carbon–diamondlike carbon (Ti-Ti_xC_y-DLC) functionally graded nanocomposite coatings, were developed to increase the fracture toughness of DLC-based coatings while preserving the superhardness (60 to 70 GPa) of DLC. The study demonstrated how the potential of superhard DLC coatings for wear protection can be multiplied by the development of functionally graded nanocomposite designs.

In this present investigation two types of wear experiment were conducted to examine the sliding wear and fretting wear properties of amorphous DLC-based functionally graded nanocomposite (a-DLC/Ti-Ti_xC_y-DLC) coatings. First, unidirectional ball-on-disk sliding friction experiments were conducted to examine the wear behavior of an a-DLC/Ti-Ti_xC_y-DLC-coated AISI 440C stainless steel disk in sliding contact with a 6-mm-diameter AISI 440C stainless steel ball at room temperature in ultrahigh vacuum (7×10^{-7} to 2×10^{-6} Pa), in dry nitrogen (<1% relative humidity), and in humid air (~50 percent relative humidity). For reference, amorphous hydrogenated carbon (H–DLC) films deposited on a-DLC/Ti-Ti_xC_y-DLC coatings were also examined in the same manner. Second, fretting wear experiments were conducted to examine the fretting wear behavior of an a-DLC/Ti-Ti_xC_y-DLC-coated flat and a titanium–6 wt% aluminum–4 wt% vanadium (Ti-6Al-4V) flat, both in contact with a 9.4-mm-diameter, hemispherical Ti-6Al-4V pin at room temperature in humid air (~50 percent relative humidity).

The a-DLC/Ti-Ti_xC_y-DLC nanocomposite coatings, consisting of an a-DLC top layer and a functionally graded Ti-Ti_xC_y-DLC underlayer, were produced on AISI 440C stainless steel substrates by the hybrid technique of magnetron sputtering and pulsed-laser deposition. The H–DLC films were produced on a-DLC/Ti-Ti_xC_y-DLC functionally graded nanocomposite coatings by the impact of an ion beam (composed of a mixture of methane (CH_4) and argon (Ar) or oxygen (O_2)) at an ion energy of 1500 or 300 eV.

The resultant a-DLC- and H–DLC-based, functionally graded, nanocomposite coatings and their wear surfaces were characterized by Raman spectroscopy, scanning electron microscopy (SEM), energy-dispersive x-ray spectroscopy (EDX), and surface profilometry. Raman spectroscopy was used to characterize the carbon bonding and the chemical structure. SEM and EDX were used to determine the morphology and elemental composition of wear surfaces and wear debris. The sampling depth of EDX for elemental information ranged between 0.5 and 1 mm in this investigation. Surface profilometry was used to determine the surface morphology, roughness, and wear of the coatings.

MATERIALS

Figure 1(a), a schematic diagram of the a-DLC/Ti-Ti_xC_y-DLC functionally graded nanocomposite coating, also shows the composition and properties of the coating layers. Voevodin et al. (ref. 15) provides detailed analyses of the gradations of compositional, structural, and mechanical properties in the graded coating. The coating composition varied from titanium to a-DLC through an intermediate Ti_xC_y ceramic region, and the hardness generally increased gradually from the AISI 440C stainless steel substrate to the a-DLC, preventing sharp changes in chemistry, structure, and mechanical properties.

The a-DLC/Ti-Ti_xC_y-DLC multilayer coatings were prepared with a hybrid technology called magnetron-sputter-assisted, pulsed-laser deposition (MSPLD) (ref. 16). Fluxes of energetic carbon from pulsed-laser deposition and titanium atoms from magnetron sputtering were intersected on the substrate surface. The individual fluxes were controlled independently to achieve a preprogrammed variation of the composition and structure across the coating thickness. Laser beam scanning and specimen positioning ensured a uniform coating without compositional variations in directions parallel to the substrate surface. All depositions were performed with substrate temperatures of 100 °C. The substrates were AISI 440C stainless steel disks (3 mm thick, 25 mm in diameter) heat treated to the Vickers microhardness of 7 to 8 GPa and polished to below 0.1-μm centerline-average roughness (R_a). They were etched with 1 keV argon ions for 30 min prior to deposition. The functionally graded nanocomposite coating comprised an ~0.5-μm-thick DLC layer on a 0.45-μm-thick graded Ti-Ti_xC_y-DLC underlayer. Six specimens of a-DLC/Ti-Ti_xC_y-DLC functionally graded nanocomposite coatings deposited on AISI 440C stainless steel disk substrates were used in this investigation. Their surfaces were smooth and their centerline-average roughness (R_a), measured by using a cutoff of 1 mm, was 19 nm with a standard deviation of 5 nm.

Figure 1(b) is a schematic diagram of an H–DLC film deposited on an a-DLC/Ti-Ti_xC_y-DLC functionally graded nanocomposite underlayer. The H–DLC films (ref. 17) were produced on the underlayer by the impact of an ion beam composed of a 3:17 mixture of Ar and CH_4 at an ion energy of 1500 eV, a 1:17 mixture of O_2 and CH_4 at an ion energy of 1500 eV, and a 2:17 mixture of O_2 and CH_4 at an ion energy of 300 eV (table I). The H–DLC film

thickness and centerline-average roughness (R_a), measured by using a cutoff of 1 mm, as well as the radiofrequency power used are also presented in table I. The H–DLC films contained more than 30 percent hydrogen (ref. 18).

Figure 2 presents typical Raman spectra of an a-DLC/Ti-Ti_xC_y-DLC functionally graded nanocomposite coating and an H–DLC film deposited on the a-DLC/Ti-Ti_xC_y-DLC coating. The two Raman spectra are similar and indicate the presence of amorphous nondiamond carbon both in the a-DLC top layer and in the H–DLC film, but the characteristic sp^3-bonded diamond peak is absent. The two spectra show that sp^2-bonded graphitic amorphous carbon was prevalent in both the a-DLC and H–DLC.

The polished Ti-6Al-4V flats were smooth; the mean R_a, measured by using a cutoff of 0.8 mm, was 7.3 nm with a standard deviation of 0.94 nm. The surfaces of the 6-mm-diameter AISI 440C stainless steel balls (grade 10) were smooth (mean R_a, 25 nm). The polished surfaces of the 9.4-mm-diameter hemispherical Ti-6Al-4V pins were also smooth (mean R_a, 110 nm).

EXPERIMENTS

Unidirectional ball-on-disk sliding friction experiments were conducted in ultrahigh vacuum (7×10^{-7} to 2×10^{-6} Pa), in dry nitrogen (<1 percent relative humidity), and in humid air (~50 percent relative humidity) at 23 °C (table II). All sliding experiments were conducted with a load of 0.98 N at a constant rotating speed of 120 rev/min (the sliding velocity ranged from 31 to 107 mm/s because of the wear track radii involved in the experiments). The friction-and-wear apparatus used in the investigation (fig. 3(a)) was mounted in a vacuum chamber. The apparatus can measure friction in ultrahigh vacuum, in dry nitrogen, and in humid air during sliding. Wear was quantified by measuring the size of the wear scar and wear track on each specimen after the wear experiment. All sliding experiments were conducted with 6-mm-diameter AISI 440C stainless steel balls in sliding contact with a-DLC/Ti-Ti_xC_y-DLC functionally graded nanocomposite coatings deposited on AISI 440C stainless steel substrate disks and with H–DLC films deposited on the a-DLC/Ti-Ti_xC_y-DLC coatings. The initial mean Hertzian contact pressure was ~0.6 GPa. The friction force was continuously monitored during the experiments. Coating wear volumes were obtained by measuring the average cross-sectional area, determined from stylus tracings, across the wear tracks at a minimum of eight locations in each wear track. Then, the average cross-sectional area of the wear track was multiplied by the wear track length. The wear rate, known as the dimensional wear coefficient, is defined as the volume of material removed at a unit load and in a unit sliding distance expressed as cubic millimeters/newton-meter.

Fretting wear experiments were conducted in humid air (~50 percent relative humidity) at 23 °C (table II). All fretting wear experiments were conducted with a load of 1.47 N at a constant frequency of 80 Hz with an amplitude of 75 μm for a total of 500 000 cycles. The fretting wear apparatus used in the investigation (fig. 3(b)) was mounted in a closed chamber. All fretting wear experiments were conducted with 9.5-mm-diameter hemispherical Ti-6Al-4V pins in contact with Ti-6Al-4V flats and in contact with a-DLC/Ti-Ti_xC_y-DLC functionally graded nanocomposite coatings deposited on AISI 440C stainless steel substrate disks. The initial mean Hertzian contact pressures were ~0.25 and 0.35 GPa, respectively.

RESULTS AND DISCUSSION

Sliding Friction and Wear of a-DLC and H–DLC

Friction behavior.—Figure 4 presents typical friction traces obtained in ultrahigh vacuum, in dry nitrogen, and in humid air for a-DLC/Ti-Ti_xC_y-DLC functionally graded nanocomposite coatings and for H–DLC films deposited on these coatings, both in sliding contact with AISI 440C stainless steel balls, as a function of the number of passes to 10 000. The friction traces indicate the marked difference in friction due to the environmental conditions and the materials pairs.

With the a-DLC (fig. 4(a)) the mean coefficients of friction obtained in ultrahigh vacuum were higher than those obtained in dry nitrogen and in humid air by factors of 3 to 10. Also, the irregularities in the friction traces were much greater in ultrahigh vacuum than in dry nitrogen and humid air. The steady-state coefficients of friction obtained in dry nitrogen after 3000 passes were slightly higher than those obtained in humid air. With a-DLC (amorphous carbon), as with graphite, the water vapor in humid air can reduce friction.

With the H–DLC (fig. 4(b)) the mean coefficients of friction obtained in ultrahigh vacuum after ~500 passes were higher than those obtained in dry nitrogen and in humid air by factors of 2 to 17. Also, the irregularities in the friction traces were much greater in ultrahigh vacuum than in dry nitrogen and humid air. The high friction and its variations resulted from high adhesion. The coefficients of friction obtained in humid air to 10 000 passes were much higher than those obtained in dry nitrogen. With the H–DLC friction rose with the presence of water vapor in humid air, opposite to the effect of water vapor on a-DLC's friction.

Figure 5 presents friction traces obtained in ultrahigh vacuum for an a-DLC/Ti-Ti_xC_y-DLC functionally graded nanocomposite coating and for an H–DLC film deposited on this coating, both in sliding contact with AISI 440C stainless steel balls, as a function of the number of passes to 1000 and 670 passes, respectively. The coefficients of friction were lower for the H–DLC than for the a-DLC by a factor of 6. The mean steady-state coefficient of friction for the H–DLC was relatively low, ~0.1 from 60 to 630 passes. The a-DLC had a high coefficient of friction, ~0.6 to 1000 passes. After 630 passes the coefficient of friction for the H–DLC increased to 0.3 at 670 passes because the H–DLC film was locally removed and the a-DLC/Ti-Ti_xC_y-DLC underlayer was locally present on the wear track. Thus, amorphous hydrogenated carbon (H–DLC or a-C:H) markedly reduced friction in ultrahigh vacuum.

Wear behavior.—The wear of a-DLC/Ti-Ti_xC_y-DLC functionally graded nanocomposite coatings in sliding contact with an AISI 440C stainless steel ball was markedly different in the different environments (ref. 19). The wear behavior of H–DLC films deposited on a-DLC/Ti-Ti_xC_y-DLC coatings was analogous to that of a-DLC/Ti-Ti_xC_y-DLC.

With the materials pair of a-DLC/Ti-Ti_xC_y-DLC coating and AISI 440C stainless steel ball, the ultrahigh vacuum caused relatively mild wear with burnishing in the a-DLC top layer to ~1200 passes. The a-DLC top layers had a mean wear rate of 4.2×10^{-6} mm^3/N-m and a coefficient of friction of 0.56 under the relatively mild wear condition (fig. 6(a)). The wear rate of the counterpart material, the AISI 440C stainless steel ball, to 1200 passes was on the order of 10^{-7} mm^3/N-m (fig. 6(b)). The a-DLC layer started to delaminate at ~1200 passes. This number is the critical number of passes to delaminate the a-DLC top layer and corresponds to the wear life of the top layer sliding against the AISI 440C stainless steel. After ~1200 passes the ultra-high-vacuum environment caused relatively severe wear with brittle fracture in both the a-DLC top layer and the Ti-Ti_xC_y-DLC underlayer, and both the coating wear rate and the coefficient of friction increased (ref. 19). Fracturing, delamination, and fragmentation of the a-DLC top layer and the Ti-Ti_xC_y-DLC underlayer took place during this relatively severe wear process in ultrahigh vacuum. After 4400 to 6500 passes the a-DLC top layer was almost completely removed from the wear track, and sliding contact between the Ti-Ti_xC_y-DLC underlayer and the AISI 440C stainless steel ball occurred. To 10 000 passes under this relatively severe wear condition, the coating wear rate and coefficient of friction were 3.0×10^{-5} mm^3/N-m and 0.92, respectively (fig. 6(a)), and the ball wear rate was 1.2×10^{-6} mm^3/N-m (fig. 6(b)).

The dry-nitrogen and humid-air environments caused mild wear with burnishing in the a-DLC top layer. The a-DLC top layer was present in the entire track even at 550 000 sliding passes, providing a low coefficient of friction, low coating wear rate, and low ball wear rate.

H–DLC films deposited on a-DLC/Ti-Ti_xC_y-DLC nanocomposite coatings behaved much like the a-DLC/Ti-Ti_xC_y-DLC. To a critical number of passes (~600), corresponding to the wear life of the H–DLC film, the ultrahigh-vacuum environment caused relatively mild wear with burnishing in the H–DLC film. After the critical number of passes the ultra-high-vacuum environment caused relatively severe wear with brittle fracture in both the H–DLC film and the a-DLC/Ti-Ti_xC_y-DLC underlayer. In ultrahigh vacuum the H–DLC film wear rates and coefficients of friction were 9.1×10^{-7} mm^3/N-m and 0.1 and 1×10^{-6} mm^3/N-m and 0.3 to 600 and 10 000 passes, respectively (fig. 6(a)), and the ball wear rates were 8×10^{-7} and 4.7×10^{-6} mm^3/N-m to 600 and 10 000 passes, respectively (fig. 6(b)).

The dry-nitrogen and humid-air environments caused mild wear with burnishing in the H–DLC film. The H-DLC film was present in the entire track even at 550 000 sliding passes in both environments, providing a low coefficient of friction, low coating wear rate, and low ball wear rate (fig. 6).

Fretting Wear of a-DLC

On the metal surfaces of the hemispherical Ti-6Al-4V pins and the Ti-6Al-4V flats fretted in air at 50 percent relative humidity, the damage consisted of pits filled with loose oxide debris, smeared debris, and agglomerated wear debris (fig. 7). In contrast, the materials pair of Ti-6Al-4V pin and a-DLC/Ti-Ti_xC_y-DLC-coated AISI 440C

disk had remarkably different fretting scars (fig. 8). The SEM photomicrographs presented in figures 7 and 8 clearly indicate the marked difference in fretting damage resulting from the different materials pairs.

The size of the fretting wear scars (fig. 9), the degree of surface roughness developed in the pits, and the debris produced were all much less for the materials pair of Ti-6Al-4V and a-DLC than for the materials pair of Ti-6Al-4V and Ti-6Al-4V. The a-DLC coating remarkably reduced the area of surface fretting damage—by a factor of 18 for the pin and by a factor of 11 for the flat.

The surface roughness in the surface-damaged area of the Ti-6Al-4V flat after contact with the Ti-6Al-4V pin (fig. 10(a)) was 51 times greater than that of the not-fretted, polished area. But, the surface roughness in the fretting scar of the a-DLC flat after contact with the Ti-6Al-4V pin (fig. 10(a)) was almost the same order of magnitude as the surface roughness of the not-fretted, as-deposited coating surface. The mean value of maximum fretting scar depth in the Ti-6Al-4V flats in contact with the Ti-6Al-4V pins was 28 times greater than that in the a-DLC flats in contact with Ti-6Al-4V pins (fig. 10(b)).

CONCLUDING REMARKS

The friction and wear of a-DLC/Ti-Ti_xC_y-DLC functionally graded nanocomposite coatings differed markedly for different environmental conditions and materials pairs. The humid-air and dry-nitrogen environments caused mild wear with burnishing in the a-DLC top layer, but the ultra-high-vacuum environment caused relatively severe wear with brittle fracture in both the a-DLC top layer and the Ti-Ti_xC_y-DLC underlayer. The humid-air and dry-nitrogen environments provided a preferable level of low coefficient of friction, low wear rate of the a-DLC top layer, and low wear rate of the AISI 440C stainless steel ball (counterpart material).

Hydrogenated carbon (H–DLC) markedly reduced friction in ultrahigh vacuum. H–DLC films deposited on a-DLC/Ti-Ti_xC_y-DLC nanocomposite coatings behaved much like the a-DLC/Ti-Ti_xC_y-DLC coatings in dry nitrogen and in humid air, providing low coefficient of friction, low coating wear rate, and low ball wear rate.

A marked difference in fretting damage resulted with different materials pairs: the materials pair of a-DLC/Ti-Ti_xC_y-DLC-coated AISI 440C stainless steel disk and AISI 440C stainless steel ball was superior in fretting wear and damage resistance to the materials pair of Ti-6Al-4V and itself. The a-DLC/Ti-Ti_xC_y-DLC functionally graded coating remarkably reduced the fretting damage on the surfaces of both a-DLC and AISI 440C stainless steel.

REFERENCES

1. A.A. Voevodin, S.D. Walck, and J.S. Zabinski, *Wear*, 203–204 (1997) 516–527.
2. K. Holmberg, H. Ronkainen, and A. Matthews, *New Directions in Tribology*, Institution of Mechanical Engineers, London, 1997, pp. 251–268.
3. D.V. Fedoseev, S.N. Dub, I.N. Lupich, and B.A. Maslyuk, *Diamond Relat. Mater.*, 1, 5–6 (1992) 543–545.
4. M.D. Bentzon, K. Mogensen, J. Bindslev Hansen, and C. Barholm-Hansen, *Surf. Coat. Technol.*, 68–69 (1994) 651–655.
5. J. Koskinen, H. Ronkainen, J.-P. Hirvonen, R. Lappalainen, and K.A. Pischow, *Diamond Relat. Mater.*, 4, 5–6 (1995) 843–847.
6. H. Kupfer, F. Richter, S. Friedrich, and Spies, H.J., *Surf. Coat. Technol.*, 74–75, 1–3 (1995) 333–338.
7. D. Li, X.-W. Lin, S.-C. Cheng, V.P. Dravid, Y.W. Chung, M.-S. Wong, and W.D.Sproul, *Appl. Phys. Lett.*, 68, 9 (1996) 1211–1213.
8. K. Miyoshi, R.L.C. Wu, and W.C. Lanter, *Tribol. Lett.*, 3, 2 (1997) 141–145.
9. A.A. Voevodin, M.S. Donley, J.S. Zabinski, and J.E. Bultman, *Surf. Coat. Technol.*, 76–77, 1–3 (1995) 534–539.
10. H. Dimigen and C.-P. Klages, *Surf. Coat. Technol.*, 49, 1–3 (1991) 543–547.
11. A.A. Voevodin, R. Bantle, and A. Matthews, *Wear*, 185, 1–2 (1995) 151–157.
12. A.A. Voevodin, C. Rebholz, and A. Matthews, *Tribol. Trans.*, 38, 4 (1995) 829–836.
13. R.L.C. Wu, K. Miyoshi, R. Vuppuladhadium, and H.E. Jackson, *Surf. Coat. Technol.*, 54–55, 1–3 (1992) 576–580.
14. K. Miyoshi, J.J. Pouch, and S.A. Alterovitz, *Mater. Sci. Forum*, 52–53, (1989) 645–656.

15. A.A. Voevodin, M.A.Capano, S.J.P. Laube, M.S. Donley, and J.S.Zabinski, *Thin Sol. Films*, 298, 1–2 (1997) 107–115.
16. A.A. Voevodin, M.A.Capano, A.J. Safriet, M.S. Donley, and J.S.Zabinski, *Appl. Phys. Lett.*, 69, 2 (1996) 188–190.
17. R.L.C. Wu, W. Lanter, K. Miyoshi, S.L. Heidger, P. Bletzinger, and A. Garscadden, *Proceedings of Beam-Solid Interactions for Materials Synthesis and Characterization Symposium*, Materials Research Society, Pittsburgh, PA, 1995, pp. 63–68.
18. K. Miyoshi, R.L.C. Wu, and W. C. Lanter, *Tribol. Lett.*, 3, 2 (1997) 141–145.
19. K. Miyoshi and K.W. Street, Friction and Wear Properties of a-DLC-Based Functionally Graded Nanocomposite Coatings. NASA/TM—1998-206962, 1998.

TABLE I.—DEPOSITION CONDITIONS, THICKNESS, AND SURFACE ROUGHNESS OF H-DLC FILMS DEPOSITED ON a-DLC/Ti-Ti_xC_y-DLC COATINGS BY DIRECT IMPACT OF ION BEAM
[Room temperature.]

Gas mixture	Ion energy, eV	Radio-frequency power, W	Thickness, nm	Surface roughness, R_a, nm	
				Mean	Standard deviation
Ar (3) CH_4 (17)	1500	91	800	10	1.7
O_2(1) CH_4(17)	1500	79	400	22	5.4
O_2(2) CH_4(17)	300	79	260	35	6.7

TABLE II.—CONDITIONS FOR SLIDING WEAR AND FRETTING WEAR EXPERIMENTS

Condition	Unidirectional, pin-on-disk, rotating sliding friction experiments	Fretting wear experiments
Environment	Humid air (~50 percent relative humidity (RH)) Dry nitrogen (<1 percent RH) Ultrahigh vacuum (7×10^{-7} to 2×10^{-6} Pa)	Humid air (50 percent RH)
Substrate	AISI 440C stainless steel disk	AISI 440C stainless steel disk
Coating	a-DLC/Ti-Ti_xC_y-DLC H-DLC/a-DLC/Ti-Ti_xC_y-DLC	a-DLC/Ti-Ti_xC_y-DLC
Flat	- - - - - - - - - - - - - - - - - - - -	Ti-6Al-4V flat
Counterpart material	6-mm-diameter AISI 440C stainless steel ball (grade 10)	9.4-mm-diameter hemispherical Ti-6Al-4V pin
Load, N	0.98	1.57
Contact pressure, GPa	0.6	0.25 for Ti-6Al-4V on Ti-6Al-4V 0.35 for Ti-6Al-4V on a-DLC coating
Rotating speed, rpm	120	- - - - - - - - - - - - - - - - - - - -
Sliding velocity, mm/s	31 to 107	- - - - - - - - - - - - - - - - - - - -
Frequency, Hz	- - - - - - - - - - - - - - - - - - - -	80
Amplitude, μm	- - - - - - - - - - - - - - - - - - - -	75
Total number of cycles	- - - - - - - - - - - - - - - - - - - -	500 000

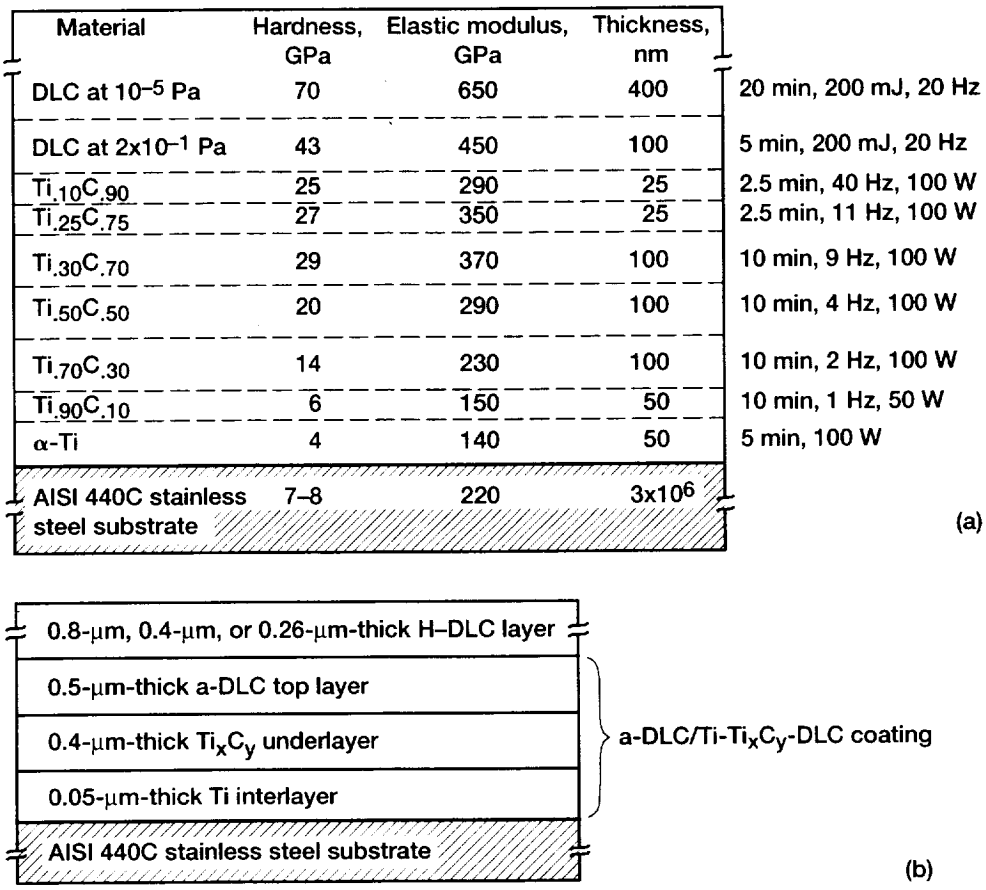

Figure 1.—Schematic diagram of a-DLC and H–DLC coatings. (a) Functionally graded a-DLC/Ti-TixCy-DLC multilayer coating showing gradation of composition and properties across coating thickness. (b) H–DLC coatings deposited on a-DLC/Ti-TixCy-DLC.

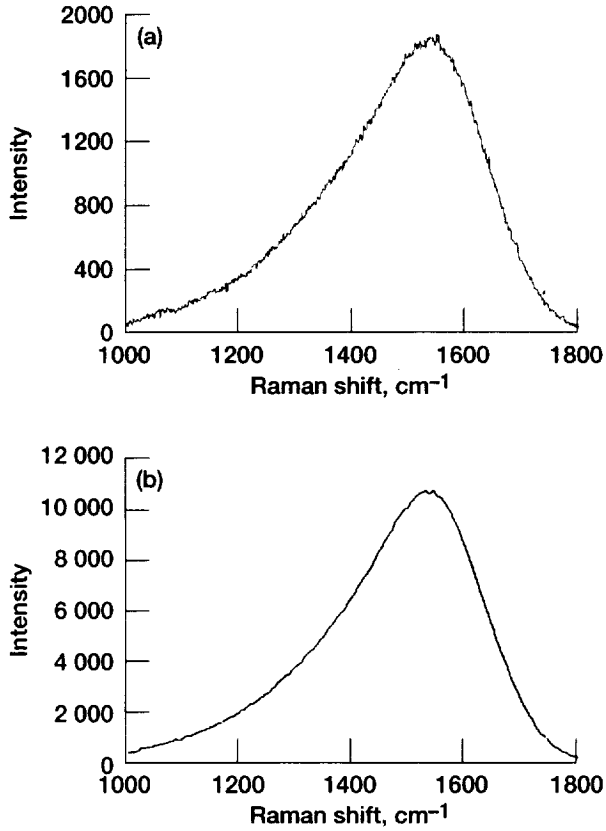

Figure 2.—Raman spectra of (a) a-DLC/Ti-TixCy-DLC coating and (b) H–DLC film.

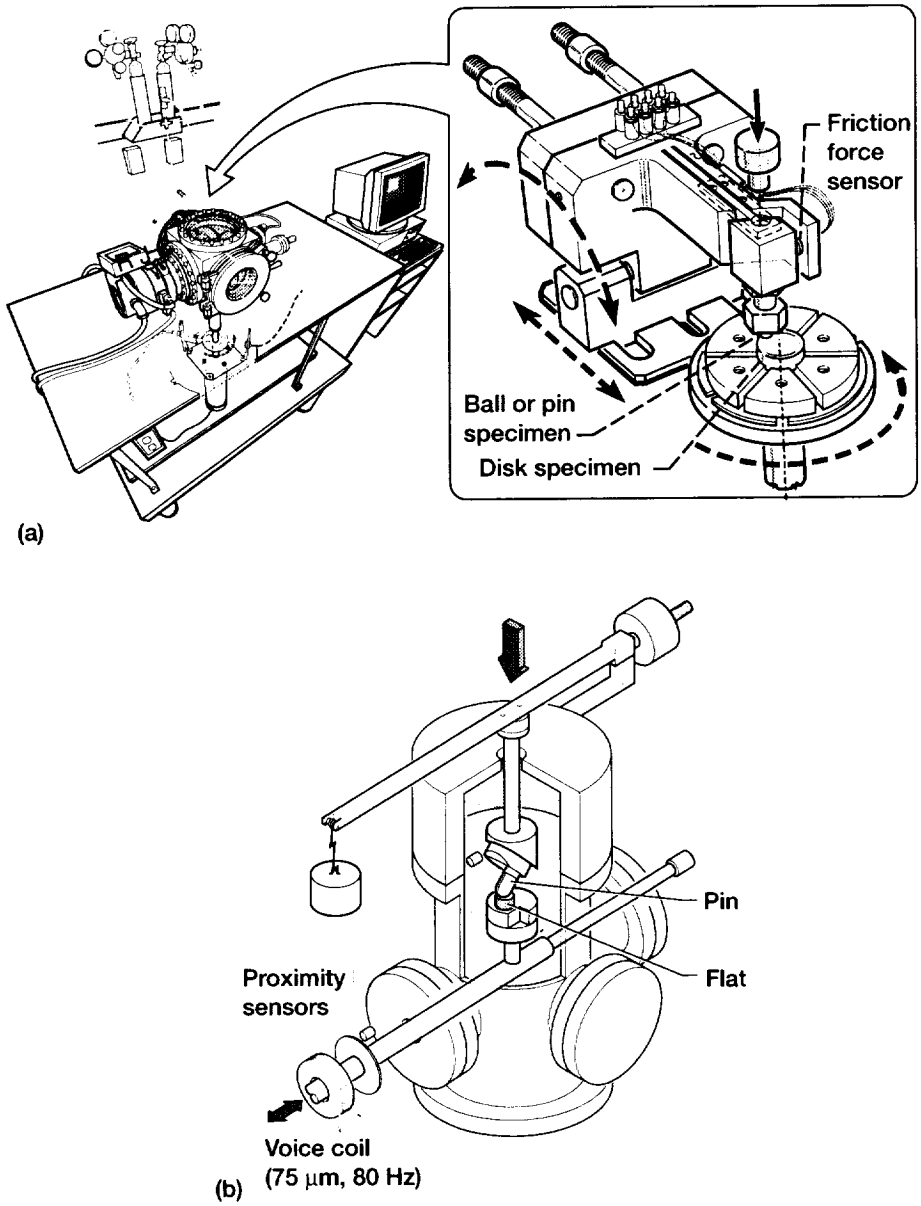

Figure 3.—Sliding and fretting wear apparatuses. (a) Pin- or ball-on-disk tribometer in vacuum chamber. (b) Fretting wear apparatus.

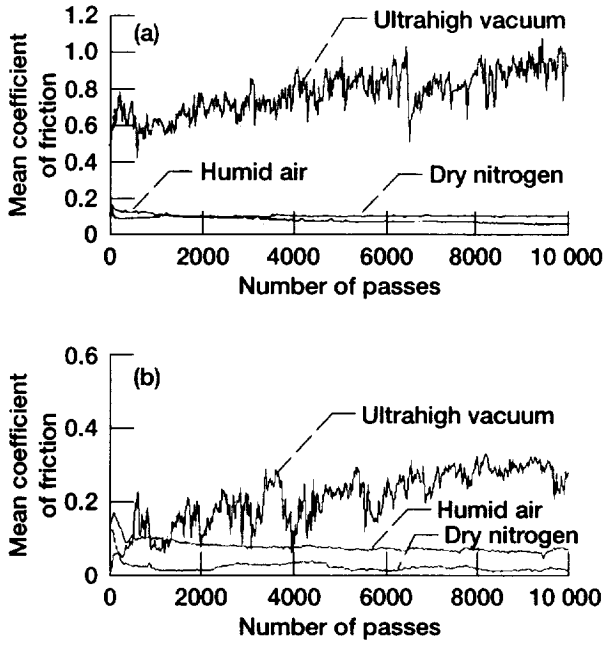

Figure 4.—Friction traces for DLC-based, functionally graded nanocomposite coatings in sliding contact with AISI 440C stainless steel balls as function of number of passes in ultrahigh vacuum, in dry nitrogen, and in humid air. (a) a-DLC/Ti-TixCy-DLC. (b) H–DLC film deposited on a-DLC/Ti-TixCy-DLC.

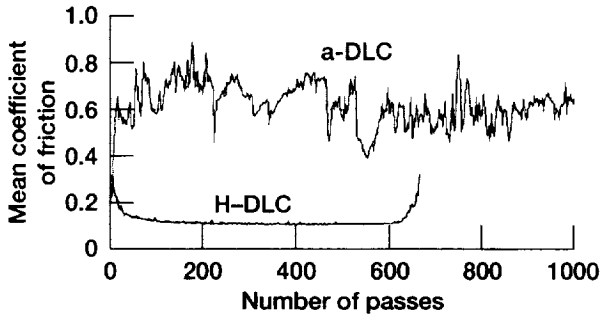

Figure 5.—Friction traces for a-DLC/Ti-TixCy-DLC coating and for H–DLC film deposited on a-DLC/Ti-TixCy-DLC in sliding contact with AISI 440C stainless steel balls as function of number of passes in ultrahigh vacuum.

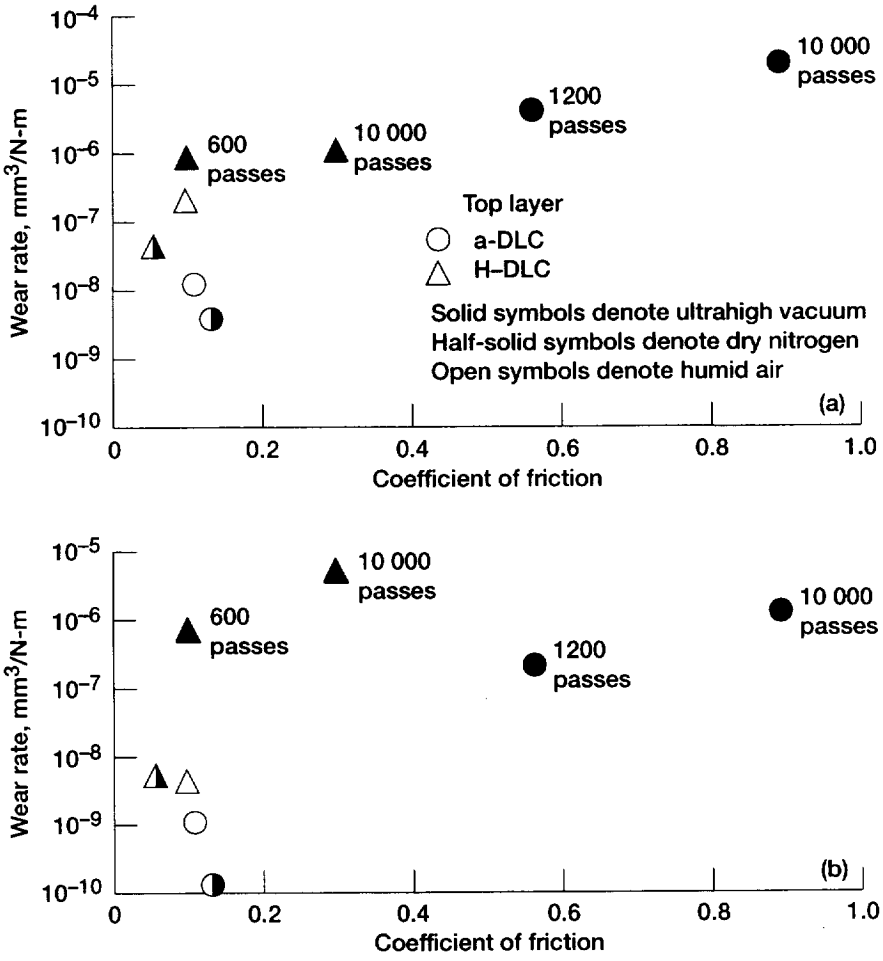

Figure 6.—Coefficients of friction and wear rates (a) for DLC coatings and (b) for AISI 440C stainless steel balls in sliding contact in ultrahigh vacuum, in dry nitrogen, and in humid air.

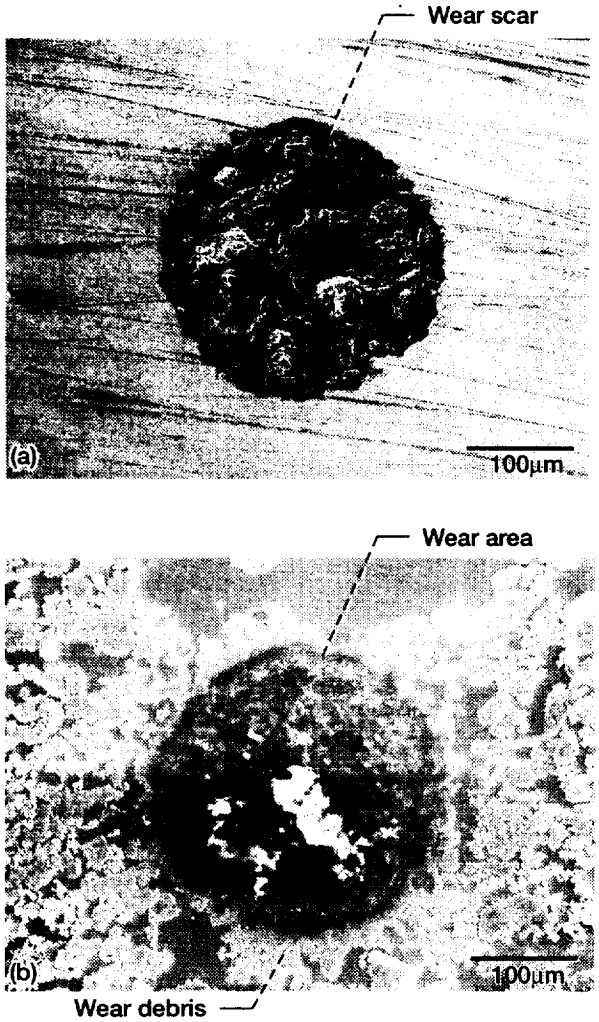

Figure 7.—Fretting wear scars (a) on Ti-6Al-4V pin and (b) on Ti-6Al-4V flat in humid air at 50% relative humidity.

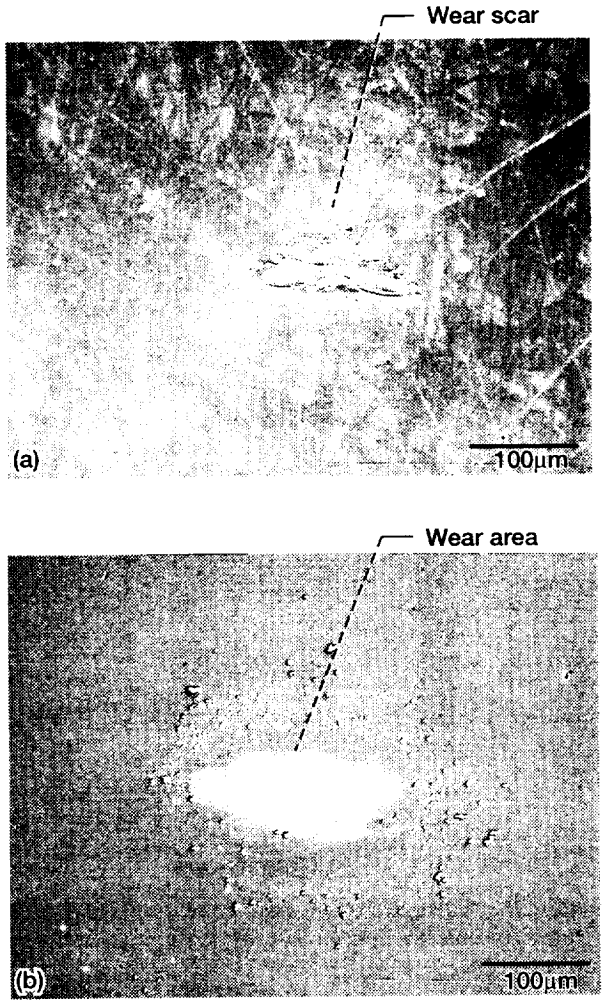

Figure 8.—Fretting wear scars (a) on Ti-6Al-4V pin and (b) on a-DLC/Ti-TixCy-DLC-coated AISI 440C disk in humid air at 50% relative humidity.

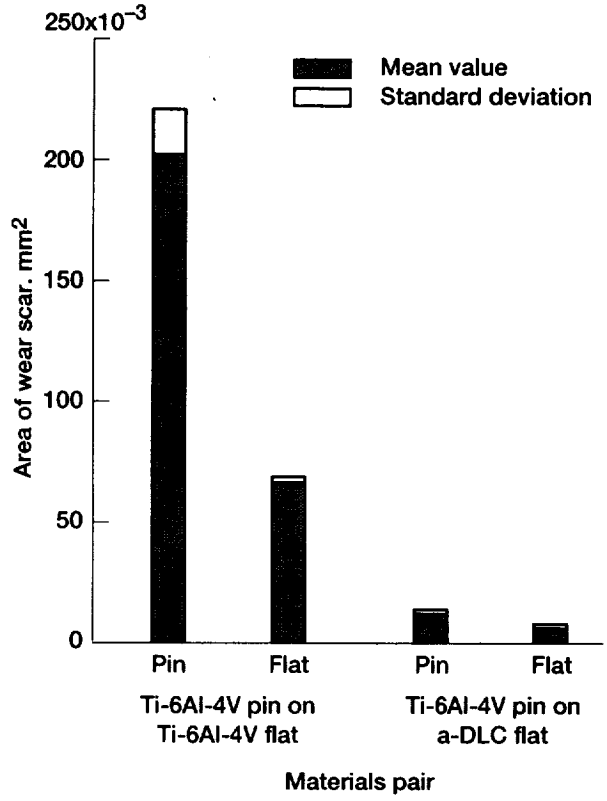

Figure 9.—Sizes of fretting wear scars for Ti-6Al-4V pin on Ti-6Al-4V flat and for Ti-6Al-4V pin on a-DLC flat.

REPORT DOCUMENTATION PAGE

Form Approved
OMB No. 0704-0188

1. AGENCY USE ONLY (*Leave blank*)	2. REPORT DATE	3. REPORT TYPE AND DATES COVERED
	May 1999	Technical Memorandum

4. TITLE AND SUBTITLE

Sliding Wear and Fretting Wear of DLC-Based, Functionally Graded Nanocomposite Coatings

5. FUNDING NUMBERS

WU–523–22–13–00

6. AUTHOR(S)

K. Miyoshi, B. Pohlchuck, Kenneth W. Street, J.S. Zabinski, J.H. Sanders, A.A. Voevodin, and R.L.C. Wu

7. PERFORMING ORGANIZATION NAME(S) AND ADDRESS(ES)

National Aeronautics and Space Administration
John H. Glenn Research Center at Lewis Field
Cleveland, Ohio 44135–3191

8. PERFORMING ORGANIZATION REPORT NUMBER

E–11250–1

9. SPONSORING/MONITORING AGENCY NAME(S) AND ADDRESS(ES)

National Aeronautics and Space Administration
Washington, DC 20546–0001

10. SPONSORING/MONITORING AGENCY REPORT NUMBER

NASA TM—1999-209076

11. SUPPLEMENTARY NOTES

K. Miyoshi, B. Pohlchuck, and Kenneth W. Street, NASA Glenn Research Center; J.S. Zabinski, J.H. Sanders, and A.A. Voevodin, Air Force Research Laboratory, Wright-Patterson Air Force Base, Ohio 45433; R.L.C. Wu, K Systems Corp., Beavercreek, Ohio 45432. Responsible person, K. Miyoshi, organization code 5140, (216) 433–6078.

12a. DISTRIBUTION/AVAILABILITY STATEMENT

Unclassified - Unlimited
Subject Category: 27 Distribution: Nonstandard

This publication is available from the NASA Center for AeroSpace Information, (301) 621–0390.

12b. DISTRIBUTION CODE

13. ABSTRACT ***(Maximum 200 words)***

Improving the tribological functionality of diamondlike carbon (DLC) films—developing good wear resistance, low friction, and high load-carrying capacity—was the aim of this investigation. Nanocomposite coatings consisting of an amorphous DLC (a-DLC) top layer and a functionally graded titanium–titanium carbon–diamondlike carbon (Ti-Ti_xC_y-DLC) underlayer were produced on AISI 440C stainless steel substrates by the hybrid technique of magnetron sputtering and pulsed-laser deposition. The resultant DLC films were characterized by Raman spectroscopy, scanning electron microscopy, and surface profilometry. Two types of wear experiment were conducted in this investigation: sliding friction experiments and fretting wear experiments. Unidirectional ball-on-disk sliding friction experiments were conducted to examine the wear behavior of an a-DLC/Ti-Ti_xC_y-DLC-coated AISI 440C stainless steel disk in sliding contact with a 6-mm-diameter AISI 440C stainless steel ball in ultrahigh vacuum, dry nitrogen, and humid air. Although the wear rates for both the coating and ball were low in all three environments, the humid air and dry nitrogen caused mild wear with burnishing in the a-DLC top layer, and the ultrahigh vacuum caused relatively severe wear with brittle fracture in both the a-DLC top layer and the Ti-Ti_xC_y-DLC underlayer. For reference, amorphous hydrogenated carbon (H–DLC) films produced on a-DLC/Ti-Ti_xC_y-DLC nanocomposite coatings by using an ion beam were also examined in the same manner. The H–DLC films markedly reduced friction even in ultrahigh vacuum without sacrificing wear resistance. The H–DLC films behaved much like the a-DLC/Ti-Ti_xC_y-DLC nanocomposite coating in dry nitrogen and humid air, presenting low friction and low wear. Fretting wear experiments were conducted in humid air (approx. 50% relative humidity) at a frequency of 80 Hz and an amplitude of 75 mm on an a-DLC/Ti-Ti_xC_y-DLC-coated AISI 440C disk and on a titanium–6 wt% aluminum–4 wt% vanadium (Ti-6Al-4V) flat, both in contact with a 9.4-mm-diameter, hemispherical Ti-6Al-4V pin. The resistance to fretting wear and damage of the a-DLC/Ti-6Al-4V materials pair was superior to that of the Ti-6Al-4V/Ti-6Al-4V materials pair.

14. SUBJECT TERMS

Coating; Tribology; Materials

15. NUMBER OF PAGES

21

16. PRICE CODE

A03

17. SECURITY CLASSIFICATION OF REPORT	18. SECURITY CLASSIFICATION OF THIS PAGE	19. SECURITY CLASSIFICATION OF ABSTRACT	20. LIMITATION OF ABSTRACT
Unclassified	Unclassified	Unclassified	

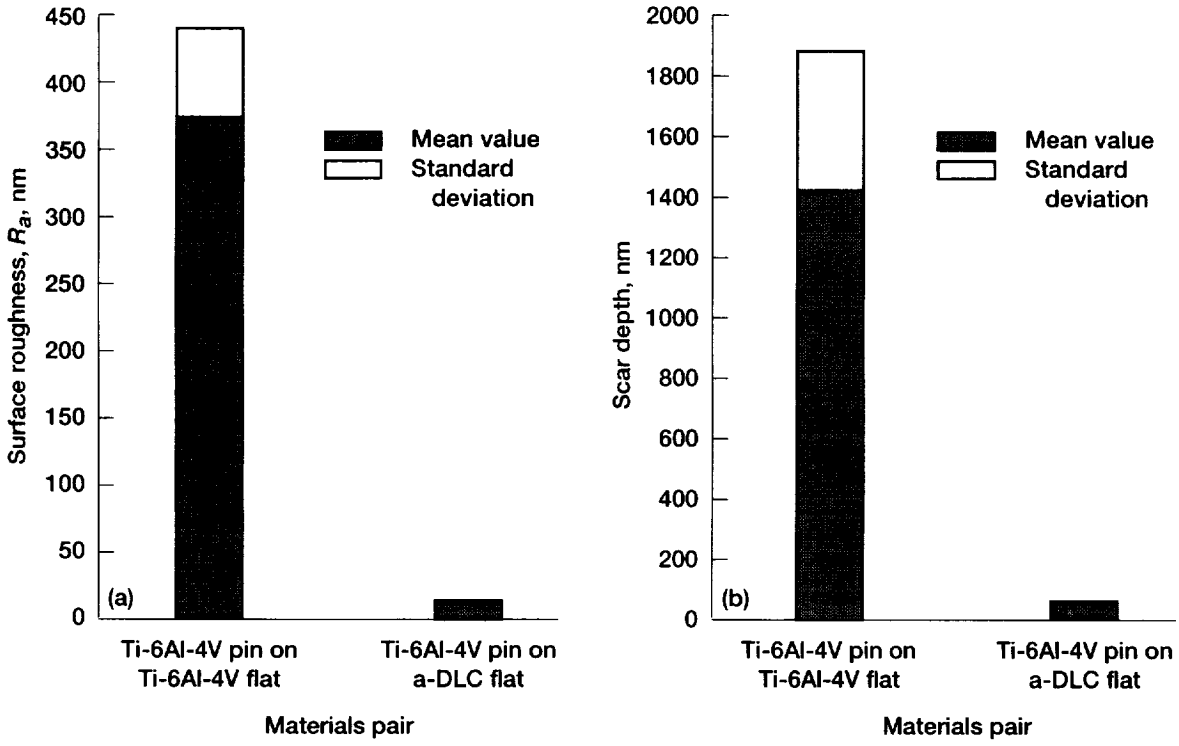

Figure 10.—Surface roughness developed in fretting wear scars and maximum depth of fretting wear scars for Ti-6Al-4V/a-DLC materials pair. (a) Surface roughness of fretting scars on flat. (b) Maximum depth of fretting scars on flat.